Journal of Zhejiang University SCIENCE
ISSN 1009-3095
http://www.zju.edu.cn/jzus
E-mail: jzus@zju.edu.cn

Semi-active control of a cable-stayed bridge under multiple-support excitations

DAI Ze-bing (代泽兵)†, HUANG Jin-zhi (黄金枝), WANG Hong-xia (王红霞)

(*School of Civil Engineering and Mechanics, Shanghai Jiaotong University, Shanghai 200240, China*)

†E-mail: zbdaicn@163.com

Received Mar. 4, 2003; revision accepted Aug. 18, 2003

Abstract: This paper presents a semi-active strategy for seismic protection of a benchmark cable-stayed bridge with consideration of multiple-support excitations. In this control strategy, Magnetorheological (MR) dampers are proposed as control devices, a LQG-clipped-optimal control algorithm is employed. An active control strategy, shown in previous researches to perform well at controlling the benchmark bridge when uniform earthquake motion was assumed, is also used in this study to control this benchmark bridge with consideration of multiple-support excitations. The performance of active control system is compared to that of the presented semi-active control strategy. Because the MR fluid damper is a controllable energy- dissipation device that cannot add mechanical energy to the structural system, the proposed control strategy is fail-safe in that bounded-input, bounded-output stability of the controlled structure is guaranteed. The numerical results demonstrated that the performance of the presented control design is nearly the same as that of the active control system; and that the MR dampers can effectively be used to control seismically excited cable-stayed bridges with multiple-support excitations.

Key words: Cable-stayed bridge, Multiple-support excitation, MR damping, Semi-active control
Document code: A **CLC number:** U448.27; TU311.3

INTRODUCTION

Although many efforts were made over the past decades to understand the dynamic behavior of cable-stayed bridges (Wilson and Gravelle, 1991), very little has been reported in the literature about their seismic response-control analysis. Even in those studies reported, only uniform earthquake motion was assumed along the entire bridge (Ni and Spencer, 2000; Jung *et al*., 2001; Yozo, 2002). This assumption, however, may be unrealistic for long span bridges since the differences in ground motion among different supports due to traveling seismic waves may result in quantitative and qualitative differences in seismic response as compared with those produced by uniform motion at all supports (Aly, 1992; Aspasia, 1990).

The control of long-span bridges represents a challenging and unique problem, with many complexities in modeling, control design and implementation. Cable-stayed bridges exhibit complex behavior in which the vertical, translational and torsional motions are often strongly coupled. It is clear that the control of very flexible bridge structures has not been studied to the same extent as buildings have (Dyke *et al*., 2000).

In order to make structural properties more adaptive to responses, many control algorithms and devices in the field of civil engineering have been investigated over the last two decades with the aim to protect structures against strong earthquakes. Passive control systems are relatively simple and easy to be complemented, but the effectiveness of passive devices is limited due to their passive nature and the random nature of earthquake events. Active control systems can offer the advantage of being able to dynamically modify the response of a structure in order to increase its safety and reliability. However, the engineering community has not yet fully embraced this technology because of questions of cost effectiveness, reliability, power requirements, etc.

An alternative approach is the semi-active control device offering the reliability of passive devices, yet maintaining the versatility and adaptability of fully active systems. Because semi-active control systems are inherently stable and require relatively much less power, application of semi-active control systems to civil engineering structures is very promising. Magnetorheological (MR) fluid dampers developed recently (Spencer *et al*., 1997) can be controlled with small power supplies; and the dynamic range of the damping force is quite large. Consequently, full-scale implementation of semi-active control with MR fluid dampers becomes a possible solution.

The focus of this paper is to use the benchmark bridge model of Dyke *et al*.(2000) to investigate the effectiveness of MR damping strategies for seismic protection of cable-stayed bridges under multiple-support excitation. In this study, MR fluid dampers are considered as supplemental damping devices, and a LQG-clipped-optimal control algorithm, shown to perform well in previous studies (Dyke *et al*., 1996; Jung *et al*., 2001) is employed. Since an MR damper is an energy-dissipative device that cannot add mechanical energy to the structural system, the proposed control strategy guarantees the bounded-input, bounded-output stability of the controlled structure. Following an overview of the benchmark, including discussion of the benchmark bridge model and evaluation criteria, a dynamic formulation of bridge with multiple-support excitations and a control system design using MR damping strategies are proposed. Numerical simulation results are then presented to demonstrate the effectiveness of the proposed control strategy.

BENCHMARK PROBLEM STATEMENTS

To effectively study the seismic response control of cable-stayed bridges and direct future research efforts toward the most promising control strategies, a benchmark structural control problem for seismically excited cable-stayed bridges was developed under the coordination of the ASCE Task Committee on Structural Control Benchmarks (Dyke *et al*., 2000; Caicedo *et al*., 2002).

This benchmark problem considers the cable-stayed bridge shown in Fig.1, which is currently under construction in Cape Griardeau, Missouri, USA. Based on detailed drawings of the bridge, a three-dimensional linear evaluation model has been developed to represent the complex behavior of the full-scale benchmark bridge. Since this bridge is assumed to be attached to bedrock, the effect of the soil-structure interaction has been neglected.

Eighteen criteria were defined (Dyke *et al*., 2000) to evaluate the capabilities of each proposed control strategy. Three historical earthquake records are considered, the 1940 El Centro NS (North-South), the 1985 Mexico City NS, and the 1999 Gebze NS.

The following first six evaluation criteria con-

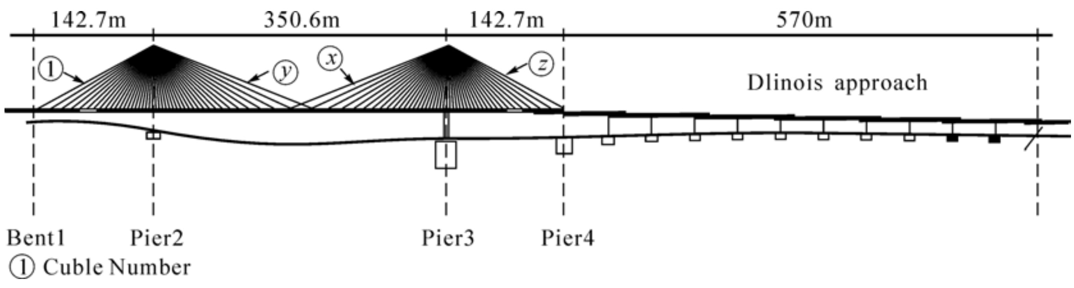

Fig.1 Schematic of the Cape Girardeau Bridge

sider the ability of the controller to reduce peak responses:

$$J_1 = \max_{\substack{\text{EI\_centro}\\ \text{Mexico\_city}\\ \text{Gebze}}} \left\{ \frac{\max_{i,t} |F_{bi}(t)|}{F_{0b}^{\max}} \right\},$$

$$J_2 = \max_{\substack{\text{EI\_centro}\\ \text{Mexico\_city}\\ \text{Gebze}}} \left\{ \frac{\max_{i,t} |F_{di}(t)|}{F_{0d}^{\max}} \right\},$$

$$J_3 = \max_{\substack{\text{EI\_centro}\\ \text{Mexico\_city}\\ \text{Gebze}}} \left\{ \frac{\max_{i,t} |M_{bi}(t)|}{M_{0b}^{\max}} \right\},$$

$$J_4 = \max_{\substack{\text{EI\_centro}\\ \text{Mexico\_city}\\ \text{Gebze}}} \left\{ \frac{\max_{i,t} |M_{di}(t)|}{M_{0d}^{\max}} \right\},$$

$$J_5 = \max_{\substack{\text{EI\_centro}\\ \text{Mexico\_city}\\ \text{Gebze}}} \left\{ \max_{i,t} \left| \frac{T_{ai}(t) - T_{0i}}{T_{0i}} \right| \right\},$$

$$J_6 = \max_{\substack{\text{EI\_centro}\\ \text{Mexico\_city}\\ \text{Gebze}}} \left\{ \max_{i,t} \left| \frac{x_{bi}(t)}{x_{0b}} \right| \right\}.$$

where $F_{bi}(t)$ is the base shear at the ith tower, $F_{0b}^{\max} = \max|F_{0bi}(t)|$. is the maximum uncontrolled base shear, $F_{di}(t)$ is the shear at the deck level in the ith tower, $F_{0d}^{\max} = \max|F_{0di}(t)|$ is the maximum uncontrolled shear at the deck level, $M_{bi}(t)$ is the moment at the base of the tower, $M_{0b}^{\max} = \max|M_{0bi}(t)|$ is the maximum uncontrolled moment at the base of the two towers, $M_{di}(t)$ is the moment at the deck level in the ith tower, $M_{0d}^{\max} = \max|M_{0di}(t)|$ is the maximum uncontrolled moment at the deck level in the two towers, $T_{0i}(t)$ is the nominal pretension in the ith cable, $T_{ai}(t)$ is the actual tension in the cable, $x_{bi}(t)$ is the displacement of the bridge deck at the ith location and x_{0b} is the maximum of the uncontrolled deck response at these locations.

The second five evaluation criteria consider normed (i.e., root mean square (RMS)) responses over the entire simulation time as follows:

$$J_7 = \max_{\substack{\text{EI\_centro}\\ \text{Mexico\_city}\\ \text{Gebze}}} \left\{ \frac{\max_{i} \|F_{bi}(t)\|}{\|F_{0b}(t)\|} \right\},$$

$$J_8 = \max_{\substack{\text{EI\_centro}\\ \text{Mexico\_city}\\ \text{Gebze}}} \left\{ \frac{\max_{i} \|F_{di}(t)\|}{F_{0d}(t)} \right\},$$

$$J_9 = \max_{\substack{\text{EI\_centro}\\ \text{Mexico\_city}\\ \text{Gebze}}} \left\{ \frac{\max_{i} \|M_{bi}(t)\|}{M_{0b}(t)} \right\},$$

$$J_{10} = \max_{\substack{\text{EI\_centro}\\ \text{Mexico\_city}\\ \text{Gebze}}} \left\{ \frac{\max_{i} \|M_{di}(t)\|}{M_{0d}(t)} \right\},$$

$$J_{11} = \max_{\substack{\text{EI\_centro}\\ \text{Mexico\_city}\\ \text{Gebze}}} \left\{ \max_{i} \frac{\|T_{ai}(t) - T_{0i}\|}{T_{0i}} \right\},$$

$$\|\cdot\| = \sqrt{\frac{1}{t_f} \int_0^{t_f} (\cdot)^2 \mathrm{d}t} .$$

where $\|F_{0b}(t)\|$ is the maximum RMS uncontrolled base shear of the two towers, $\|F_{0d}(t)\|$ is the maximum RMS uncontrolled shear at the deck level, $\|M_{0b}(t)\|$ is the maximum RMS uncontrolled overturning moment of the two towers, $\|M_{0d}(t)\|$ is the maximum RMS uncontrolled moment at the deck level.

The last seven evaluation criteria consider the requirements of each control system itself:

$$J_{12} = \max_{\substack{\text{EI\_centro}\\ \text{Mexico\_city}\\ \text{Gebze}}} \left\{ \max_{i,t} \left(\frac{f_i(t)}{W} \right) \right\},$$

$$J_{13} = \max_{\substack{\text{EI\_centro}\\ \text{Mexico\_city}\\ \text{Gebze}}} \left\{ \max_{i,t} \left(\frac{y_i^{d}(t)}{x_0^{\max}} \right) \right\},$$

$$J_{14} = \max_{\substack{\text{EI\_centro}\\ \text{Mexico\_city}\\ \text{Gebze}}} \left\{ \frac{\max_{t} \left[\sum_i P_i(t) \right]}{\dot{x}_0^{\max} W} \right\},$$

$$J_{15} = \max_{\substack{\text{EI\_centro}\\ \text{Mexico\_city}\\ \text{Gebze}}} \left\{ \frac{\sum_i \left(\int_0^{t_f} P_i(t) \mathrm{d}t \right)}{x_0^{\max} W} \right\},$$

J_{16} = Number of control devices,

J_{17} = Number of sensors,

$J_{18} = \dim(\boldsymbol{x}_k^{\mathrm{c}})$

where $f_i(t)$ is the force generated by the ith control device over the time history, W=510 000 kN is the seismic weight of a bridge based on the mass of the superstructure, $y_i^{\mathrm{d}}(t)$ is the stroke of the ith control device, $x_0^{\max}$ is the maximum uncontrolled displacement at the top of the towers relative to the ground, $P_i(t)$ is a measure of the instantaneous power required by the ith control device, and $\boldsymbol{x}_k^{\mathrm{c}}$ is the discrete-time state vector of the control algorithm.

DYNAMIC FORMULATION OF BRIDGE SUBJECTED TO MULTI-SUPPORT EXCITATIONS

Considering the general equation of motion for a cable-stayed bridge subjected to uniform seismic loads, the dynamic function can be written as

$$\boldsymbol{M}\ddot{\boldsymbol{U}} + \boldsymbol{C}\dot{\boldsymbol{U}} + \boldsymbol{K}\boldsymbol{U} = -\boldsymbol{M}\boldsymbol{\Gamma}\ddot{\boldsymbol{x}}_{\mathrm{g}} + \boldsymbol{\Lambda}\boldsymbol{f} \tag{1}$$

where $\boldsymbol{U}$ is the displacement response vector, $\boldsymbol{M}$, $\boldsymbol{C}$ and $\boldsymbol{K}$ are the mass, damping and stiffness matrices of the structure, $\boldsymbol{f}$ is the vector of control force inputs, $\ddot{\boldsymbol{x}}_{\mathrm{g}}$ is the longitudinal ground acceleration, $\boldsymbol{\Gamma}$ is a vector of zeros and ones relating the ground acceleration to the bridge degrees of freedom (DOF), and $\boldsymbol{\Lambda}$ is a vector relating the force (s) produced by the control device (s) to the bridge DOFs.

This is appropriate when the excitation has a single component or when the excitation is uniformly applied at all supports of the structure. For the analysis of the bridge with multiple-support excitation, however, the model must include the degrees of freedom at the supports. The equation of dynamic equilibrium for all the DOFs is written in partitioned form (Caicedo *et al*., 2002)

$$\begin{aligned}&\begin{bmatrix}\boldsymbol{M} & \boldsymbol{M}_{\mathrm{g}}\\ \boldsymbol{M}_{\mathrm{g}}^{\mathrm{T}} & \boldsymbol{M}_{\mathrm{gg}}\end{bmatrix}\begin{bmatrix}\ddot{\boldsymbol{U}}^{1}\\ \ddot{\boldsymbol{U}}_{\mathrm{g}}\end{bmatrix}+\begin{bmatrix}\boldsymbol{C} & \boldsymbol{C}_{\mathrm{g}}\\ \boldsymbol{C}_{\mathrm{g}}^{\mathrm{T}} & \boldsymbol{C}_{\mathrm{gg}}\end{bmatrix}\begin{bmatrix}\dot{\boldsymbol{U}}^{1}\\ \dot{\boldsymbol{U}}_{\mathrm{g}}\end{bmatrix}\\ &+\begin{bmatrix}\boldsymbol{K} & \boldsymbol{K}_{\mathrm{g}}\\ \boldsymbol{K}_{\mathrm{g}}^{\mathrm{T}} & \boldsymbol{K}_{\mathrm{gg}}\end{bmatrix}\begin{bmatrix}\boldsymbol{U}^{1}\\ \boldsymbol{U}_{\mathrm{g}}\end{bmatrix}=\begin{bmatrix}\boldsymbol{0}\\ \boldsymbol{P}_{\mathrm{g}}\end{bmatrix}+\begin{bmatrix}\boldsymbol{\Lambda}\boldsymbol{f}\\ \boldsymbol{0}\end{bmatrix}\end{aligned} \tag{2}$$

where $\boldsymbol{U}^{1}$ and $\boldsymbol{U}_{\mathrm{g}}$ are the absolute displacement vector of the superstructure and the displacement vector of the supports, respectively. Matrices $\boldsymbol{M}$, $\boldsymbol{C}$ and $\boldsymbol{K}$ are the system matrices of the supper structure. Matrices $\boldsymbol{M}_{\mathrm{g}}$, $\boldsymbol{C}_{\mathrm{g}}$ and $\boldsymbol{K}_{\mathrm{g}}$ are the mass, damping and elastic-coupling matrices expressing the forces developed in the active DOFs by the motion of the supports. Matrices $\boldsymbol{M}_{\mathrm{gg}}$, $\boldsymbol{C}_{\mathrm{gg}}$, $\boldsymbol{K}_{\mathrm{gg}}$ are the mass, damping and stiffness matrices of the supports, respectively. It is desired to determine the displacement vector $\boldsymbol{U}^{1}$ in the superstructure DOFs and the support forces $\boldsymbol{P}_{\mathrm{g}}$.

The total displacement $\boldsymbol{U}^{1}$ is expressed as quasi-static displacement $\boldsymbol{U}^{\mathrm{s}}$, plus the dynamic displacement $\boldsymbol{U}$, i.e.

$$\boldsymbol{U}^{1} = \boldsymbol{U}^{\mathrm{s}} + \boldsymbol{U} \tag{3}$$

and

$$\begin{bmatrix}\boldsymbol{K} & \boldsymbol{K}_{\mathrm{g}}\end{bmatrix}\begin{bmatrix}\boldsymbol{U}^{\mathrm{s}} & \boldsymbol{U}_{\mathrm{g}}\end{bmatrix}^{\mathrm{T}} = \boldsymbol{0} \tag{4}$$

Define the pseudo-static influence vector $\boldsymbol{R}_{\mathrm{s}}$ as

$$\boldsymbol{R}_{\mathrm{s}} = -\boldsymbol{K}^{-1}\boldsymbol{K}_{\mathrm{s}} \tag{5}$$

Substituting Eqs.(3), (4) and (5) into the first line of Eq.(2) gives

$$\begin{aligned}\boldsymbol{M}\ddot{\boldsymbol{U}} + \boldsymbol{C}\dot{\boldsymbol{U}} + \boldsymbol{K}\boldsymbol{U} =& \boldsymbol{\Lambda}\boldsymbol{f} - (\boldsymbol{M}\boldsymbol{R}_{\mathrm{s}} + \boldsymbol{M}_{\mathrm{g}})\ddot{\boldsymbol{U}}_{\mathrm{g}}\\ &-\left(\boldsymbol{C}\boldsymbol{R}_{\mathrm{s}} + \boldsymbol{C}_{\mathrm{g}}\right)\dot{\boldsymbol{U}}_{\mathrm{g}}\end{aligned} \tag{6}$$

If the ground accelerations and velocities are prescribed at each support, this completes the formulation of the governing equation. Eq.(6) can be rewritten in state space form as

$$\dot{\boldsymbol{x}} = \boldsymbol{A}_{\mathrm{e}}\boldsymbol{x} + \boldsymbol{B}_{\mathrm{e}}\begin{bmatrix}\ddot{\boldsymbol{U}}_{\mathrm{g}}\\ \dot{\boldsymbol{U}}_{\mathrm{g}}\\ \boldsymbol{f}\end{bmatrix} \tag{7}$$

Where $\boldsymbol{x}=\begin{bmatrix}\boldsymbol{U}^{\mathrm{T}} & \dot{\boldsymbol{U}}^{\mathrm{T}}\end{bmatrix}^{\mathrm{T}}$ is the state vector,

$$\boldsymbol{A}_{\mathrm{e}}=\begin{bmatrix}\mathbf{0} & \mathbf{0}\\ -\boldsymbol{M}^{-1}\boldsymbol{K} & -\boldsymbol{M}^{-1}\boldsymbol{C}\end{bmatrix},$$

$$\boldsymbol{B}_{\mathrm{e}}=\begin{bmatrix}\mathbf{0}\\ \boldsymbol{M}^{-1}\begin{bmatrix}-\boldsymbol{M}\boldsymbol{R}_{\mathrm{s}}-\boldsymbol{M}_{\mathrm{g}} & -\boldsymbol{C}\boldsymbol{R}_{\mathrm{s}}-\boldsymbol{C}_{\mathrm{g}} & \boldsymbol{\Lambda}\end{bmatrix}\end{bmatrix}$$

MR FLUID DAMPERS

Because of their mechanical simplicity, high dynamic range, low power requirements, large force capacity and robustness, MR dampers have been shown to mesh well with application demands and constraints to offer an attractive means of protecting civil infrastructure systems against severe earthquake and wind loading (Dyke *et al.*, 1996; Jansen and Dyke, 2000).

Many types of dynamic models for MR fluid dampers have been investigated by researchers. One of them, denoted as modified Bouc-Wen model (Fig.2), proposed by Spencer *et al.*(1997), has been shown to accurately predict the behavior of the prototype MR damper over a broad range of inputs. The equations governing the force predicted by this model are:

$$f=c_1\dot{y}+k_1(x-x_0) \tag{8}$$

$$\dot{y}=\frac{1}{(c_0+c_1)}\{\alpha z+c_0\dot{x}+k_0(x-y)\} \tag{9}$$

$$\dot{z}=-\gamma\left|\dot{x}-\dot{y}\right|z\left|z\right|^{n-1}-\beta(\dot{x}-\dot{y})\left|z\right|^{n}+A(\dot{x}-\dot{y}) \tag{10}$$

where x is the displacement of the damper; k_1= accumulator stiffness; c_0 = viscous damping at large velocities; c_1 = viscous damping for force roll-off at low velocities; k_0 = stiffness at large velocities; and x_0 = initial displacement of spring k_1. By adjusting the parameters of the model γ, β, A, n, one can control the linearity in the unloading and the smoothness of the transition from the preyield to the postyield region. The latter three parameters depend on the command voltage u to the current driver

$$\begin{aligned}\alpha&=\alpha(u)=\alpha_{\mathrm{a}}+\alpha_{\mathrm{b}}u\\ c_0&=c_0(u)=c_{0\mathrm{a}}+c_{0\mathrm{b}}u\\ c_1&=c_1(u)=c_{1\mathrm{a}}+c_{1\mathrm{b}}u\end{aligned} \tag{11}$$

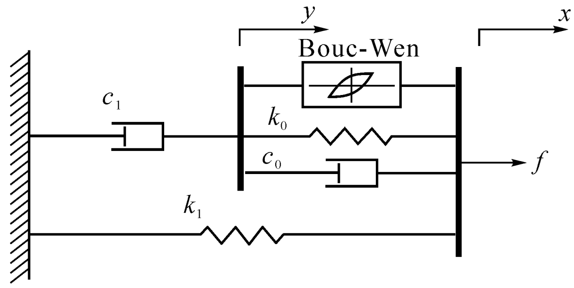

Fig.2 Simple mechanical model of the MR damper

In addition, the dynamics involved in the MR fluid reaching rheological equilibrium are accounted for through the first order filter

$$\dot{u}=-\eta(u-v) \tag{12}$$

where v is the command voltage applied to the control circuit.

In this study, the parameters of the MR damper were selected so that the device has a capacity of 1000 kN, as follows: α_a=46.2 kN/m, α_b=41.2 kN/m /V, c_{0a}=110.0 kN·s/m, c_{0b}=114.3 kN·s/m/V, c_{1a} =8359.2 kN·s/m, c_{1b}=7842.9 kN·s/m/V, η=100, k_0=0.002 kN/m, k_1=0.0097 kN/m, x_0=0.0 m, γ= 164.0 m^{-2}, β=164.0 m^{-2}, A=1107.2, n=2. These parameters are based on the experimental results of a 20-ton MR damper (Yang *et al.*, 2002) and scaled up to have maximum capacity of 1000 kN with maximum applied voltage $V_{\max}$=10 Volts.

SEMI-ACTIVE CONTROL STRATEGY USING MR DAMPER

Many researchers have investigated various types of control algorithms for semi-active control. The performance of the LQG-clipped optimal control algorithm was found to be close to that obtained from the active control by linear optimal control

(Jansen and Dyke, 2000).

In the LQG-clipped-optimal controller, the approach is to append *n* force feedback loops to induce each MR damper to produce approximately a desired control force. The desired control force of the *i*th MR damper is denoted. A linear optimal controller is designed that calculates a vector of desired control forces, based on the measured structural response vector and the measured control force vector, i.e.,

$$\boldsymbol{f}_{\mathrm{c}} = L^{-1}\left\{-\boldsymbol{K}_{\mathrm{c}}(s)L\begin{Bmatrix}\boldsymbol{y}_{\mathrm{m}}\\ \boldsymbol{f}_{\mathrm{m}}\end{Bmatrix}\right\} \tag{13}$$

where $L\{\}$ is the Laplace transform. $\boldsymbol{y}_{\mathrm{m}}$ is the measured structural response vector and $\boldsymbol{f}_{\mathrm{m}}$ is the measured control force vector. $\boldsymbol{K}_{\mathrm{c}}(s)$ is the linear optimal controller. Although the controller can be obtained from a variety of synthesis methods, H_2/LQG strategies are advocated herein because of the stochastic nature of earthquake ground motions and because of their successful application in other civil engineering structural control applications (Dyke et al., 1996).

The algorithm for selecting the command signal for the ith MR damper can be concisely stated as

$$v_i = V_{\max} H(\{f_{ci} - f_{mi}\} f_{mi}) \tag{14}$$

where $V_{\max}$ is the maximum voltage to the current driver, and $H()$ is Heaviside step function. Further discussion of this control algorithm is provided in Dyke et al.(1996).

DESIGN OF THE NOMINAL CONTROLLER

The LQG-clipped-optimal control algorithm and active control algorithm are based on a nominal controller design. Here an H_2/LQG control algorithm is employed for the nominal controller. The controller is designed using the reduced order model (i.e., design model) of the system, which is derived from the evaluation model by forming a balanced realization of the system and condensing out the states with relatively small controllability and observability grammians as follows

$$\dot{\boldsymbol{x}}_{\mathrm{r}} = \boldsymbol{A}_{\mathrm{r}}\boldsymbol{x}_{\mathrm{r}} + \boldsymbol{B}_{\mathrm{r}}\begin{bmatrix}\ddot{\boldsymbol{U}}_{\mathrm{g}}\\ \dot{\boldsymbol{U}}_{\mathrm{g}}\end{bmatrix} + \boldsymbol{E}_{\mathrm{r}}\boldsymbol{f} \tag{15}$$

$$\boldsymbol{z} = \boldsymbol{C}_{\mathrm{r}}\boldsymbol{x}_{\mathrm{r}} + \boldsymbol{D}_{\mathrm{r}}\begin{bmatrix}\ddot{\boldsymbol{U}}_{\mathrm{g}}\\ \dot{\boldsymbol{U}}_{\mathrm{g}}\end{bmatrix} + \boldsymbol{F}_{\mathrm{r}}\boldsymbol{f} \tag{16}$$

$$\boldsymbol{y}_{\mathrm{m}} = \boldsymbol{C}_{\mathrm{m}}\boldsymbol{x}_{\mathrm{r}} + \boldsymbol{D}_{\mathrm{m}}\begin{bmatrix}\ddot{\boldsymbol{U}}_{\mathrm{g}}\\ \dot{\boldsymbol{U}}_{\mathrm{g}}\end{bmatrix} + \boldsymbol{F}_{\mathrm{m}}\boldsymbol{f} \tag{17}$$

where $\boldsymbol{x}_r$ is the vector of regulated responses, and $\boldsymbol{z}$ is the regulated output vector.

In the design of the H_2/LQG controller, the disturbances to the system (i.e., $\begin{bmatrix}\ddot{\boldsymbol{U}}_{\mathrm{g}}^{\mathrm{T}} & \dot{\boldsymbol{U}}_{\mathrm{g}}^{\mathrm{T}}\end{bmatrix}^{\mathrm{T}}$), are taken to be identically distributed, statistically independent stationary white noise processes, and $S_{\mathrm{w}} = S_{\mathrm{ww}} I_{8\times 8}$, and an infinite horizon performance index is chosen as

$$J = \lim_{\tau\to\infty}\frac{1}{\tau}E[\int_0^{\tau}\{(\boldsymbol{C}_{\mathrm{r}}\boldsymbol{x}_{\mathrm{r}} + \boldsymbol{F}_{\mathrm{r}}\boldsymbol{f})^{\mathrm{T}}\boldsymbol{Q}(\boldsymbol{C}_{\mathrm{r}}x_{\mathrm{r}} + \boldsymbol{F}_{\mathrm{r}}\boldsymbol{f}) + \boldsymbol{f}^{\mathrm{T}}\boldsymbol{R}\boldsymbol{f}\}\mathrm{d}t] \tag{18}$$

where $\boldsymbol{Q}$ and $\boldsymbol{R}$ are weighting matrices for the vectors of regulated responses and of control forces respectively. For design purposes, the measurement noise vector, $\boldsymbol{v}$, is assumed to contain identically distributed, statically independent Gaussian white noise processes, with $S_{\mathrm{ww}} / S_{v_i v_i} = \gamma = 25$.

The Kalman Filter optimal estimator is given by

$$\dot{\hat{\boldsymbol{x}}}_{\mathrm{r}} = (\boldsymbol{A}_{\mathrm{r}} - \boldsymbol{L}\boldsymbol{C}_{\mathrm{r}})\dot{\boldsymbol{x}}_{\mathrm{r}} + [\boldsymbol{L} \quad \boldsymbol{B}_{\mathrm{r}} - \boldsymbol{L}\boldsymbol{D}_{\mathrm{r}}]\begin{bmatrix}\boldsymbol{y}_{\mathrm{m}}\\ \boldsymbol{f}_{\mathrm{m}}\end{bmatrix} \tag{19}$$

$$\boldsymbol{f}_{\mathrm{c}} = -\boldsymbol{K}\hat{\boldsymbol{x}}_{\mathrm{r}} \tag{20}$$

where $\boldsymbol{L}$ is the gain matrix for state estimator and $\boldsymbol{K}$ is the gain matrix for Linear Quadratic Regulator.

As described in the previous section, the control force determined using this algorithm is compared to the measured control force, and by using Eq.(14), the appropriate control voltage is applied to the control devices.

Note that in the case of ideal active control, the applied (measured) control forces $\boldsymbol{f}_{\mathrm{m}}$ equal the desired control force $\boldsymbol{f}_{\mathrm{c}}$. Thus Eq.(19) can be rewritten as

$$\dot{\hat{\boldsymbol{z}}}_{\mathrm{r}} = (\boldsymbol{A}_{\mathrm{r}} - \boldsymbol{B}_{\mathrm{r}}\boldsymbol{K} - \boldsymbol{L}\boldsymbol{C}_{\mathrm{r}} + \boldsymbol{L}\boldsymbol{D}_{\mathrm{r}}\boldsymbol{K})\hat{\boldsymbol{z}}_{\mathrm{r}} + \boldsymbol{L}\boldsymbol{y}_{\mathrm{m}} \tag{21}$$

And force feedback is not required to implement this algorithm.

NUMERICAL SIMULATIONS

To verify the effectiveness of the presented semi-active control design, simulations were done for the three earthquakes specified in the benchmark problem statement. In this study, a total of 24 MR dampers with maximum capacity of 1000 kN are considered, eight between the deck and pier 2, eight between the deck and pier 3, four between the deck and bent 1, and four between the deck and pier 4. Five accelerometers and four displacement transducers are used for feedback to the control algorithm. Four accelerometers are located on top of the tower legs, and one is located on the deck at mid span. Two displacement sensors are placed between the deck and pier 2, and the other two are placed between the deck and pier 3. Because the LQG-clipped-optimal control algorithm requires measurement of the control forces applied to the structure, eight force transducers are installed.

In this study, the prescribed ground motion is assumed to be identical at each support, although it is not applied simultaneously. We assume that bent 1 undergoes a specified ground motion, and the motion at the other there supports is identical to the motion but delayed base on the distance between adjacent supports and the speed of the L-wave of a typical earthquake (3 km/s) (Clough and Penzien, 1993).

To evaluate the ability of the MR dampers to achieve the performance of a comparable fully active control system, the active controller considered herein is assumed to be ideal, in that actuator/sensor dynamics are not considered. The active controller is designed as Eq.(21).

As seen from Eq.(18), appropriate selection of parameters ($\boldsymbol{z}$, $\boldsymbol{Q}$, $\boldsymbol{R}$) is important in the design of the control algorithm (both active and semi-active system). In this study, $\boldsymbol{R}$ is selected as an [8×8] identity matrix; $\boldsymbol{z}$ is comprised of different responses of bridge, and accordingly $\boldsymbol{Q}$ can be selected as follows:

Case 1: deck displacement (q_{d}) and overturning moments (q_{om}) as described in Jung *et al.*(2001):

$$\boldsymbol{Q}_{\mathrm{d\&om}} = \begin{bmatrix} q_{\mathrm{d}}\boldsymbol{I}_{4\times4} & \boldsymbol{0} \\ \boldsymbol{0} & q_{\mathrm{om}}\boldsymbol{I}_{4\times4} \end{bmatrix}$$

with $q_{\mathrm{d}} = 6.7\times10^{3}$, $q_{\mathrm{om}} = 6.6\times10^{-9}$.

Case 2: deck displacement (q_{d}) and mid-span acceleration (q_{a})

$$\boldsymbol{Q}_{\mathrm{d\&a}} = \begin{bmatrix} q_{\mathrm{d}}\boldsymbol{I}_{4\times4} & \boldsymbol{0} \\ \boldsymbol{0} & q_{\mathrm{a}} \end{bmatrix} \text{ with } q_{\mathrm{d}} = 3500,\ q_{\mathrm{a}} = 350.$$

Case3: passive control without feedback $\boldsymbol{Q}_{\mathrm{zero}} = 0$ with the voltages to all MR dampers held at maximum value 10 Volts.

The weighting parameters in case 1 are shown by previous researches to perform well when earthquake motions are uniform at all supports along the entire cable-stayed bridge. As shown in the 3rd column of Table 1, however, under multiple-support excitations, the performance of the active control system with these parameters get worse dramatically over almost all of the evaluation criteria. Fortunately, with the MR dampers as control devices, as seen in the 4th column, the semi-active control system with these parameters performs much better than active control system when multiple-support excitations are considered in this bridge model. Furthermore, when the voltage of the MR damper is set to its maximum value (10 Volts) (Case 3), as shown in the last column of Table 1, the

Table 1 Maximum evaluation criteria for all the three earthquakes

	Case1			Case2		Case3
	Active uniform	Active multiple	Semi multiple	Active multiple	Semi-active multiple	Passive multiple
J_1	0.4992	0.98244	0.42854	0.49526	0.42806	0.45046
J_2	1.1988	2.49726	1.09058	0.99655	1.02299	0.82369
J_3	0.4461	0.68565	0.41847	0.43019	0.43044	0.42828
J_4	0.8692	1.67516	0.83689	0.96456	0.81627	0.52702
J_5	0.1571	0.16242	0.19427	0.15609	0.14680	0.21585
J_5	2.0181	2.41767	2.33694	2.26579	2.52846	0.99675
J_7	0.3519	4.33820	0.49898	0.54081	0.46970	0.54996
J_8	1.0118	12.48070	1.62758	1.60571	1.64715	1.26988
J_9	0.3304	2.32252	0.58724	0.62877	0.58891	0.53734
J_{10}	0.8598	7.14548	1.21260	1.21477	1.28716	0.85821
J_{11}	0.0155	0.03609	0.03272	0.03408	0.03431	0.03912
J_{12}	1.96e−3	1.9608e−3	1.9608e−3	2.9068e−3	1.9608e−3	1.5747e−3
J_{13}	1.1065	1.05496	1.01973	0.98867	1.10331	0.54280
J_{14}	9.205e−3	6.3059e−3	−	6.8329e−3	−	−
J_{15}	8.681e−4	6.2257e−4	−	6.7460e−4	−	−
J_{16}	24	24	24	24	24	24
J_{17}	9	9	9	9	9	0
J_{18}	30	60	60	60	60	60

performance gets higher than that of the semi-active control system.

As to the case 2, the performance of the LQG-clipped-optimal control system is generally similar to that of the ideal active control system as shown in Table 1. The time-history responses of the semi-active controlled bridge are compared to those of the uncontrolled bridge for the El Centro, Mexico City, and Gebze earthquakes in Fig.3, showing that the controller can achieve a significant reduction in the base shear forces as compared to the uncontrolled system.

These results verify that semi-active control strategy has nearly the same effectiveness as the active control system for seismic protection of the benchmark cable-stayed bridge model. Furthermore, if the weight parameters of the nominal controller are not selected appropriately, the control systems with MR fluid dampers perform much better than active control systems.

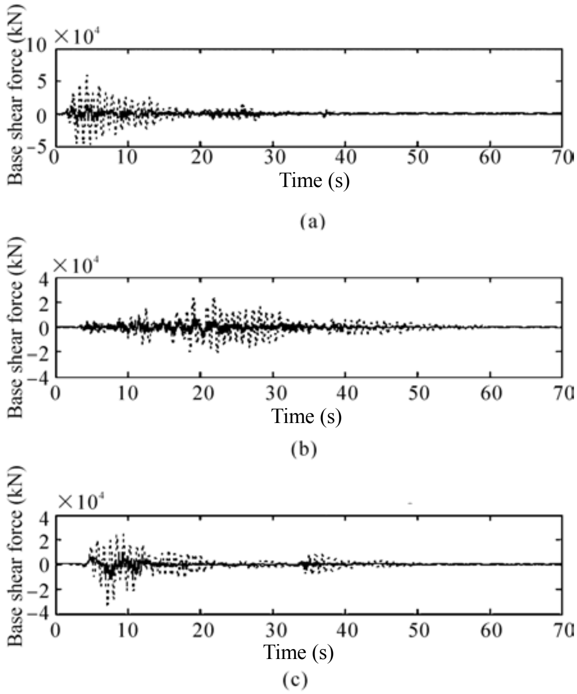

Fig.3 Historical response of uncontrolled and controlled base shear force of the benchmark bridge under 3 earthquake excitations
(a) 1940 El Centro earthquake; (b) 1998 Mexico City earthquake; (c) 1999 Gebze earthquake
.... Uncontrolled; ——— Semi-active controlled

CONCLUSION

This paper presents a semi-active control strategy using MR fluid dampers for investigating the benchmark control problem for seismic responses of cable-stayed bridges with consideration of multiple-support excitation. An LQG-clipped-optimal control algorithm is used to determine the control action for each MR fluid damper. The proposed control design employs five accelerometers, four displacement transducers and 24 force transducers as sensors, a total of 24 MR fluid dampers with a maximum capacity of 1000 kN each as control devices, and the controller has 60 states.

In comparing the active, semi-active and passive control systems, it was observed that similar performance could typically be achieved by all of these systems, reinforcing the result obtained by previous researchers that semi-active systems can achieve similar performance levels to that of active systems. In some cases the semi-active systems performed better than the active, while requiring significantly less power than the active system, especially when the weight parameters in the control algorithm are not appropriate.

In addition, semi-active control strategy has many attractive features, such as bounded-input, bounded-output stability. The results of this preliminary investigation, therefore, indicate that MR fluid dampers could effectively be used to control cable-stayed bridges subjected to multiple-support seismic excitations.

References

Aly, S.N., 1992. Effects of ground motion spatial variability on the response of cable-stayed bridges. *Earthquake engineering and structural dynamics*, **21**(1):1-20.

Aspasia, Z., 1990. Response of multi-span beams to spatially incoherent seismic ground motions. *Earthquake engineering and structural dynamics*, **19**(5):819-832.

Caicedo, J.M., Dyke, S.J., Moon, S.J., Bergman, L.A., Turan, G., Hague, S., 2002. Phase II benchmark control problem for seismic response of cable-stayed bridges (http://wusceel.cive.wustl.edu/quake/).

Dyke, S.J., Spencer, B.F., Sain, M.K., Carlson, J.D., 1996. Modeling and control of magnetorheological dampers for seismic response. *Smart Materials and Structures*, **5**:565-575.

Dyke, S.J., Turan, G., Caicedo, J.M., Bergman, L.A., Hague, S., 2000. Benchmark Control Problem for Seismic Response of Cable-Stayed Bridges (http://wusceel.civewustl.edu/quake/).

Jansen, L.M., Dyke, S.J., 2000. Semi-active control strategies for MR dampers: comparative study. *Journal of engineering Mechanics, ASCE*, **126**(8):795-803.

Jung, H.J., Spencer, B.F., Lee, I.W., 2001. Benchmark Control Problem for Seismically Excited Cable-stayed Bridges using Smart Damping Strategies. Conference on Cable-supported Bridges. Seoul, Korea, p.256-267.

Magana, M.E., Volz, P., Miller, T. 1997. Nonlinear decentralized control of a flexible cable-stayed beam structure. *ASME Journal of Vibration and Acoustics*, **119**(4): 523-526.

Ni, Y.Q., Spencer, B.F., 2000. Active/semiactive Seismic Response Control of Cable-supported Bridges: Current Research Status and Key Issues. Proceedings of the China-U.S. Millennium Symposium of Earthquake Engineering: Earthquake Engineering Frontiers in the New Millennium. Netherlands, p.229-304

Spencer, B.F., Dyke, S.J., Sain, M.K. Carlson, J.D., 1997. Phenomenological model of a magnetorheological damper. *Journal of Engineering Mechanics*, *ASCE*, **123**(3):230-238.

Wilson, J., Gravelle, W., 1991. Modelling of a cable-stayed bridge for dynamic analysis. *Earthquake Engineering and Structural Dynamics*, **20**(4):707-721.

Yang, G., Spencer, B.F., Carlson, J.D., Sain, M.K., 2002. Large-scale MR fluid dampers: modeling, and dynamic performance considerations. *Engineering structures*, **30**(3):309-323

Yozo, F., 2002. Vibration, control and monitoring of long-span bridges-resent research, developments and practice in Japan. *Journal of Constructional Steel Research*, **58**(1):71-97.